

Charge and Heat Control in Nanoelectronic Devices

A study of thermoelectric properties of quantum dots and their relation to charge and heat currents with respect to coupling strength, interaction energy, number of reservoirs and other system factors

Erik Johansson, Jakob Max
Hampus Renberg Nilsson, Selma Tabakovic

BACHELOR'S THESIS 2017:05

Charge and Heat Control in Nanoelectronic Devices

A study of thermoelectric properties of quantum dots and their relation to charge and heat currents with respect to coupling strength, interaction energy, number of reservoirs and other system factors

Erik Johansson, Jakob Max, Hampus Renberg Nilsson, Selma Tabakovic



CHALMERS
UNIVERSITY OF TECHNOLOGY

Department of Microtechnology and Nanoscience – MC2
CHALMERS UNIVERSITY OF TECHNOLOGY
Gothenburg, Sweden 2017

Charge and Heat Control in Nanoelectronic Devices

A study of thermoelectric properties of quantum dots and their relation to charge and heat currents with respect to coupling strength, interaction energy, number of reservoirs and other system factors

Erik Johansson, Jakob Max, Hampus Renberg Nilsson, Selma Tabakovic

© Erik Johansson, Jakob Max, Hampus Renberg Nilsson, Selma Tabakovic, 2017.

Supervisors: Janine Splettstößer and Fatemeh Hajiloo, Department of Microtechnology and Nanoscience – MC2

Examiner: Vessen Vassilev, Department of Microtechnology and Nanoscience – MC2

Bachelor's Thesis 2017:05

Department of Microtechnology and Nanoscience – MC2

Chalmers University of Technology

SE-412 96 Gothenburg

Telephone +46 31 772 1000

Cover: A sketch of a quantum dot system with a temperature and voltage gradient. The quantum dot is connected to two reservoirs.

Typeset in L^AT_EX

Gothenburg, Sweden 2017

Charge and Heat Control in Nanoelectronic Devices

A study of thermoelectric properties of quantum dots and their relation to charge and heat currents with respect to coupling strength, interaction energy, number of reservoirs and other system factors

Erik Johansson, Jakob Max, Hampus Renberg Nilsson, Selma Tabakovic
Department of Microtechnology and Nanoscience – MC2
Chalmers University of Technology

Abstract

This study examines thermoelectric properties in nanoelectronic devices, specifically setups known as quantum dots. Thermoelectric effects, the relation between voltage gradients and temperature biases, are investigated. Some useful thermoelectric properties of quantum dots include the ability to extract electrical power from a temperature gradient or transport heat from a cooler region to a warmer, i.e. work as a heat engine or as a heat pump. A quantum dot interacts with its environment through different terminals, e.g. a gate terminal and reservoirs. Quantum dots are an interesting setup for thermoelectric applications due to their ability to change transport properties when exposed to a gate voltage or a change in characteristics of adjoining reservoirs. The aim of this study is to find how the characteristic parameters of a quantum dot can be used to control thermoelectric effects. This is essential knowledge when designing systems where quantum dots are wanted to, for example, extract work from a heat flow. The thermoelectric effects are studied using two different methods, namely the master equation and scattering theory. Heat to work conversion and its efficiency is analysed for a set of quantum dot systems. We find the relations between parameters that makes it possible to use quantum dots to either extract electrical work from a heat bath or cool a part of the system. Furthermore, charge and heat separation is studied in a system consisting of a quantum dot, two reservoirs and a voltage probe. This is useful for managing temperatures in circuits doing electrical work. We find it is possible to separate heat and work, but that it requires a certain asymmetry in the system.

Keywords: Quantum Dot, Thermoelectric Effect, Seebeck Coefficient, Onsager Matrix, Carnot Efficiency, Master Equation, Scattering Theory, Heat to Work Conversion.

Acknowledgements

We would like to thank our supervisors Janine Splettstößer and Fatemeh Hajiloo for their outstanding commitment to our project. Not only have they always been ready to answer our questions, but also continuously met up with us to discuss our progress. We would most certainly not have gotten this far without their help, and we are very grateful for their involvement. Also, thanks for teaching us to not focus on the fork when there is cake.

Erik Johansson, Jakob Max, Hampus Renberg Nilsson, Selma Tabakovic

Contents

List of Figures	ix
Table of Definitions	x
1 Introduction	1
1.1 Background	1
1.2 Quantum Dot Systems	1
1.3 Thermoelectric Effects and Linear Coefficients	2
1.4 Efficiency of a Power Producing Quantum Dot System	3
2 Methods, Models and Properties of Quantum Dots	4
2.1 Open Quantum Systems	5
2.2 Master Equation	5
2.3 Scattering Theory	6
2.4 Models	7
2.4.1 General Properties	7
2.4.2 Currents and Coulomb Blockade Effect	8
2.4.3 Modeling a Quantum Dot Using a Double Delta Barrier	10
3 Thermoelectric Properties in the Linear Regime	10
3.1 Single Energy Level with Spinless Particles	10
3.2 Single Energy Level with Interacting Electrons	12
3.3 Non-interacting System and Strong Coupling	14
4 Thermoelectric Properties in the Non-Linear Regime	14
4.1 Single Energy Level with Spinless Electrons	15
4.2 Heat to Work Conversion	15
4.2.1 Efficiency of the Conversion	16
4.2.2 Maximize Power or Efficiency	17
4.3 Spin Degenerate Energy Level with Interacting Electrons	17
5 Charge and Heat Separation	18
5.1 Spinless Particles	18
5.2 Coulomb Interacting Electrons	18
6 Conclusions	19
Bibliography	
A Probabilities and Currents in a Magnetic Field	I
B The Transition Matrix	III

List of Figures

1	Quantum dots, in (a) a theoretical sketch with numerous reservoirs and a gate terminal and in (b) a SEM image of a real quantum dot of GaAs fabricated by electron-beam lithography with terminals labeled T, R, L and P [7].	2
2	A Fermi function and its derivative. The width of the derivative is proportional to $k_B T$	4
3	Sketch of the basic idea of scattering theory; a_α, a_β are incoming and b_α, b_β are outgoing scattering states.	6
4	Visualization of a quantum dot with two reservoirs and interacting electrons. In both figures the left reservoir has a higher temperature and higher electrochemical potential than the right reservoir. In (a) the energy level ε is inside the bias window, which allows a current to flow, while in (b) not ε nor $\varepsilon + U$ is inside the bias window which leads to Coulomb blockade.	7
5	A Coulomb diamond and particle the particle current for a quantum dot with two reservoirs with the electrochemical potentials $\mu_L = \mu_0 + \Delta\mu/2$, $\mu_R = \mu_0 - \Delta\mu/2$, the temperatures $k_B T_L = k_B T_R = 30\Gamma$ and the Coulomb interaction energy $U = 500\Gamma$. In figure 5a we see the conductance, $\partial I/\partial\Delta V$, expressed in $g_0 \equiv e^2(\Gamma_1 + \Gamma_2)/(\hbar\Gamma k_B T)$. In figure 5b we see the absolute particle current, which is proportional to the number of possible states at the same time N_ε	8
6	Probabilities for different quantum dot systems. In (a) the bias is greater than the interaction energy, i.e. $\Delta\mu > U$. In contrast in (b) the interaction energy is greater than the bias, i.e. $U > \Delta\mu$	9
7	Electrons scattered at a double delta barrier.	10
8	Conductance G and L -coefficient as functions of the position of the energy level ε , for both an interacting two-reservoir system (G_U, L_U) and a non-interacting two-reservoir system (G_0, L_0).	12
9	Fourier heat coefficient K and Seebeck coefficient S as functions of the position of the energy level ε , both in the case of an interacting two-reservoir system (K_U, S_U) and a non-interacting two-reservoir system (K_0, S_0).	13
10	A quantum dot with two reservoirs which have a temperature gradient, $T_H > T_C$ and an electrochemical gradient $\mu_H > \mu_C$. In (a) we have $\varepsilon < \varepsilon_{\text{Carnot}}$ which leads to heat to work conversion. In (b) we have ε between $\varepsilon_{\text{Carnot}}$ and $\varepsilon_{\text{cool}}$, which leads to cooling of the colder reservoir.	16
11	Produced power P and the efficiency η . The system reaches its maximum power with the efficiency η_{MP} output when $\varepsilon = \varepsilon_{\text{MP}}$. It reaches the Carnot efficiency η_{Carnot} when $\varepsilon = \varepsilon_{\text{Carnot}}$. Note that the power output at the Carnot efficiency is zero.	17
12	A weakly coupled interacting quantum dot without a bias, $\Delta\mu = 0$, but a temperature gradient, $\Delta T > 0$. ε is at $\mu_0 - U/2$ and $\varepsilon + U$ at $\mu_0 + U/2$. The particle currents cancel out but the electrons still carry heat from the warmer reservoir to the cooler.	18
13	Quantum Dot with three reservoirs, where reservoir 2 is a voltage probe.	19

Table of Definitions

$N_\alpha \equiv \langle \hat{N}_\alpha \rangle$	Expectation value of the particle number operator in reservoir α .
$I_\alpha^N \equiv -\dot{N}_\alpha$	Number of particles going <u>out</u> of reservoir α .
$I_\alpha \equiv -eI_\alpha^N$	Charge current going <u>out</u> of reservoir α .
$I_\alpha^E \equiv -\partial_t \langle \hat{H}_\alpha \rangle$	Total energy current going <u>out</u> of reservoir α , where \hat{H}_α is the Hamiltonian of reservoir α .
$J_\alpha \equiv I_\alpha^E - \mu_\alpha I_\alpha^N$	Heat current going <u>out</u> of reservoir α .
$\Gamma \equiv \sum_\alpha \Gamma_\alpha$	Sum of all the reservoirs' coupling coefficients.
$f \equiv f(\varepsilon)$	Fermi-Dirac distribution for any reservoir as a function of the energy level ε .
$f_U \equiv f(\varepsilon + U)$	Fermi-Dirac distribution for any reservoir as a function of the energy level including the interaction energy, $\varepsilon + U$.
$f_\alpha \equiv f_\alpha(\varepsilon)$	Fermi-Dirac distribution for reservoir α .
$f_{U\alpha} \equiv f_\alpha(\varepsilon + U)$	Fermi-Dirac distribution for reservoir α including the interaction energy.
$f^-, f_U^-, f_\alpha^-, f_{U\alpha}^-$	The difference between 1 and the Fermi-Dirac distributions, e.g. $f^- = 1 - f$ and $f_{U\alpha}^- = 1 - f_{U\alpha}$ and so on. This is a useful notation for increasing readability.
$f_\Sigma \equiv \sum_\alpha \Gamma_\alpha f_\alpha(\varepsilon)$	Sum of all Fermi-Dirac distributions multiplied by their corresponding Γ_α .
\vdots	\vdots

\vdots	\vdots
$f_{U\Sigma} \equiv \sum_{\alpha} \Gamma_{\alpha} f_{\alpha}(\varepsilon + U)$	Sum of all Fermi-Dirac distributions multiplied by their corresponding Γ_{α} , including the interaction energy U .
$f_{\Sigma}^{-} \equiv \Gamma - f_{\Sigma}$	Note here that f_{Σ}^{-} <u>does not</u> equal $1 - f_{\Sigma}$ due to that each Γ_{α} is included with its corresponding f_{α} in the definition of f_{Σ} .
$f_{U\Sigma}^{-} \equiv \Gamma - f_{\Sigma}$	Note here that $f_{U\Sigma}^{-}$ <u>does not</u> equal $1 - f_{U\Sigma}$ due to that each Γ_{α} is included with its corresponding $f_{U\alpha}$ in the definition of $f_{U\Sigma}$.
$\varepsilon_{\text{Carnot}}$	Value of ε for which a system has the Carnot efficiency and zero power output for heat to work conversion. Also the lower limit for cooling.
$\varepsilon_{\text{cool}}$	Maximum value of ε for which the system does cooling.

1 Introduction

This study examines the thermoelectric properties of multi-terminal nanoscale devices, in particular quantum dots. The thermoelectric properties of a system is defined by the relation between heat flow and charge current through that system. To analyse these properties, it is therefore necessary to understand how the currents that give rise to them behave. By deriving expressions for heat and electric currents, and analysing their relation to each other, the thermoelectric properties of the studied systems are examined. This is done by studying the impact of various quantum system characteristics, e.g. coupling strength and Coulomb interaction.

1.1 Background

The ongoing technical advancements in nanotechnology leads to an ever decreasing size of electronic circuits. This will eventually lead to components of a size where quantum mechanical effects will have to be considered [1]. A possible future application where this might be of interest is quantum circuits, where these quantum phenomena may be utilised to generate thermoelectric effects [2]. Quantum effects also allow for new types of functionality, for example heat to work conversion on the nanoscale [3]. In order to theoretically understand thermoelectric effects on a quantum scale, thermodynamics is no longer sufficient since it is derived by assuming macroscopic systems. To understand how systems on the smaller scale behave, new theoretical descriptions are needed [4], [5]. This opens up for many interesting research areas, as a lot of these effects are still to be analysed and understood. If this is carried out successfully, it might lead to a new era of nanoelectronic devices that can operate more quickly and efficiently than the ones we have today.

In most electric circuits, heat is an unwanted side effect that has to be dealt with. However, with knowledge of thermoelectric effects, it could also be utilised in several ways. Perhaps most important of these potential applications is conversion of waste heat into electrical work. Because of this, thermoelectric properties are interesting from a technological point of view. In components where quantum effects apply, the interaction between heat flows and charge currents are properties of significance. Efficiency of heat to work conversion is a parameter which is important to assess the usefulness of quantum thermoelectrics. In order to analyse this, one has to study how gradients of temperature and voltage influence charge and heat flow. This is essential for building optimal quantum thermoelectrics. Of particular interest is how the process efficiency relates to power output, and how these relations depend on device parameters.

1.2 Quantum Dot Systems

A so-called quantum dot is a quantum device prototype, ideal for theoretical studies. The name stems from the device being 'almost zero-dimensional', and is used to describe an electron occupied system, small enough that the energy levels of the electrons are quantized. The quantum dot is an open quantum system, meaning that the it is interacting with its reservoir environment. Quantum dots can be realized experimentally in many different ways [6], and can be used as basic building blocks for complex setups. An example of an experimental realization can be seen in figure 1b. This is a scanning electron microscope (SEM) image of a quantum dot made of GaAs and fabricated by electron-beam lithography [7].

A schematic describing a quantum dot is shown in figure 1. The potential in the dot is regulated by an applied gate voltage, and the dot can be connected to multiple reservoirs. These reservoirs are each characterized by a temperature and an electrochemical potential.

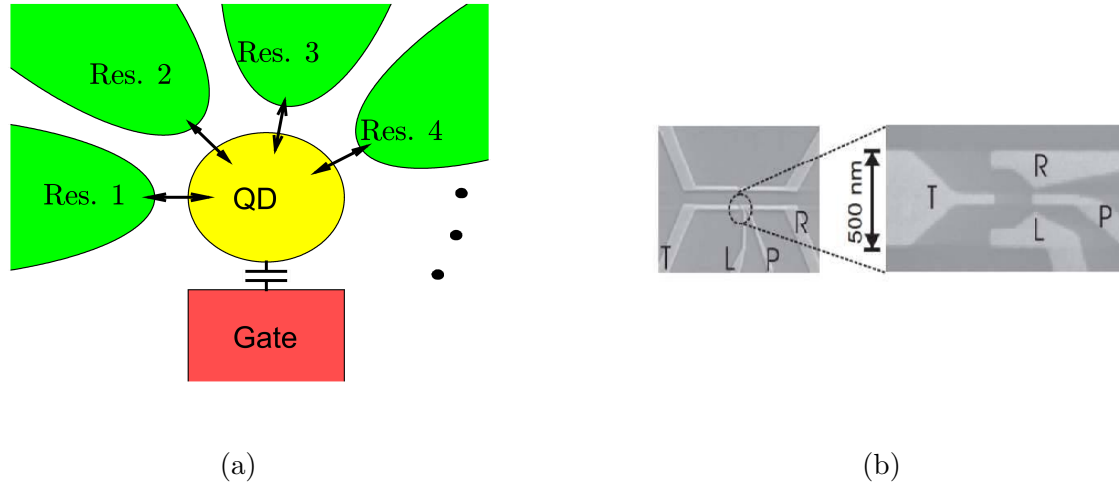


Figure 1: Quantum dots, in (a) a theoretical sketch with numerous reservoirs and a gate terminal and in (b) a SEM image of a real quantum dot of GaAs fabricated by electron-beam lithography with terminals labeled T, R, L and P [7].

Electrons can tunnel between the dot and the reservoirs. If there is a temperature gradient ΔT or a potential gradient $\Delta\mu$, the electrons are more likely to tunnel in one direction, which yields a current through the quantum dot. The probability of tunneling is often referred to as the coupling, Γ . A stronger coupling means a higher ability for the electrons to tunnel. Electrons with anti-parallel spin occupying the same energy level repel each other, and in some cases it might be interesting to investigate how this Coulomb interaction influences the behaviour of the system.

The discrete energy spectrum combined with the tunability of the energy level makes the quantum dot an interesting prototype for thermoelectric applications. By regulating the position of the energy level that can be occupied within the quantum dot, it is possible to control whether the quantum dot does *heat to work conversion*, *cooling* or *work to heat conversion*, which are three essential different thermoelectric effects.

1.3 Thermoelectric Effects and Linear Coefficients

The thermoelectric properties of a system characterises the relation between voltage and temperature gradients within it. These properties determine the relation between charge current and heat flow. Classical thermoelectrics usually consist of materials that have intrinsic thermoelectric properties, for example metal alloys such as constantan. On the contrary, the quantum dot is a device that is constructed in such a way that the quantum mechanics dictating its behaviour gives rise to thermoelectric effects, and is not a thermoelectric by its material alone. To compare the quantum dot to classical systems, we use the same quantities to describe the system, but use a quantum mechanical approach to obtain them.

Through a quantum dot there can flow a charge current I , and a heat flow J , induced by voltage and temperature gradients. The expressions for I and J are in general complicated, and difficult or impossible to calculate analytically. In section 4 we show some cases where it can be done, however these results are sometimes impractical to work with. Linear response theory can be used to simplify the charge current and heat flow to get an understanding of the thermoelectric effects for small voltage and temperature gradients. The thermoelectric effects in the linear response regime, i.e. small ΔT and ΔV ($\Delta\mu = -e\Delta V$) on the scale of

Γ , can be described by the four coefficients G, L, M and Θ . This is also referred to as the Onsager matrix [8],

$$\begin{bmatrix} I \\ J \end{bmatrix} = \begin{bmatrix} G & L \\ M & \Theta \end{bmatrix} \begin{bmatrix} \Delta V \\ \Delta T \end{bmatrix}. \quad (1)$$

This matrix gives us all information about what charge currents and heat flows are induced by voltage and temperature gradients, which is what we need to characterize the system. The coefficients G and Θ are the electrical conductance and thermal conductance respectively. They characterize the usual thermal and electric properties of the system.

The coefficients L and M are related through the *Onsager relation*

$$M = LT, \quad (2)$$

and describe thermoelectric effects. L gives the charge current in response to a temperature gradient, and M gives the heat flow caused by a voltage gradient. In equation (1) we see that when $L = 0, M = 0$, i.e. no thermoelectric effects are present, we have $I = G\Delta V$ and $J = \Theta\Delta T$, as one would expect. If L and M are non-zero, then the electric current will depend on the temperature gradient and the heat flow depends on the voltage gradient. To investigate these dependencies we introduce a few more coefficients.

The relation in equation (1) can be rewritten as

$$\begin{bmatrix} \Delta V \\ J \end{bmatrix} = \begin{bmatrix} R & -S \\ \Pi_P & K \end{bmatrix} \begin{bmatrix} I \\ \Delta T \end{bmatrix}. \quad (3)$$

In this matrix R is the regular ohmic resistance. $S = \frac{L}{G}$ is called the Seebeck coefficient, and can be interpreted as the average energy per unit charge transferred at the temperature T [3]. If we set $I = 0$, i.e. no electronic transfer, then S describes the relation between voltage and temperature gradient, $\Delta V = -S\Delta T$. This is then the condition for electric and thermal equilibrium in a thermoelectric, valid for small ΔV and ΔT . Analogously, the Peltier coefficient $\Pi_P = \frac{M}{G}$ represents the average heat carried by a unit charge. The size of S and Π_P describes how pronounced the thermoelectric effects are in a material or device. For example, in a thermocouple, a large Seebeck coefficient would mean that the voltage has a strong response to a temperature gradient, which is typically the desired behaviour for thermometer applications.

The coefficient $K = \Theta - \frac{LM}{G}$ is called the Fourier heat coefficient. It represents the thermal transport that occurs without an electron current. In the quantum dot electron tunneling is the only exchange between reservoirs that we consider, so it would seem that $K = 0$ at all times. It is, however, shown in section 3 that this is not always the case.

1.4 Efficiency of a Power Producing Quantum Dot System

Depending on the system setup, quantum dots can be used to convert heat to electrical work, i.e. work as a heat engine [8]. By reversing the power production process, turning electrical power into waste heat is also a possible outcome. This is however a process that normally occurs in most systems, and is therefore not very interesting. In addition, the quantum dot can be used for cooling, moving heat from a cold reservoir into a hotter one, by extracting work from a voltage gradient. The efficiency of heat to work conversion is given by the produced power divided by the heat absorbed from the hot reservoir, i.e.

$$\eta = \frac{-I\Delta V}{J_H}. \quad (4)$$

This expression is, as familiar, equivalent with the one for a heat engine [9]. In the setups studied here, the efficiency can also be expressed in terms of heat flows only, with $-I\Delta V = J_H + J_C$, since all heat currents are defined as positive going out of each reservoir and into the system. Thus, heat to work conversion can be achieved when more heat is flowing out of the hotter reservoir than into the colder reservoir. This efficiency should not exceed the Carnot efficiency,

$$\eta_{\text{Carnot}} = 1 - \frac{T_C}{T_H}. \quad (5)$$

Using equation (1), the efficiency in the linear regime is given by [8]

$$\eta = -\frac{G\Delta V^2 + L\Delta T\Delta V}{M\Delta V + \Theta\Delta T}. \quad (6)$$

This relations is necessary to analyse how the relations between the different thermoelectric coefficients affect the efficiency of heat to work conversion.

2 Methods, Models and Properties of Quantum Dots

Transport properties of the quantum dot are analysed with two different methods, namely the master equation and scattering theory. The transport properties determine the electric current and heat flow through the system, and the relation between them. The particle current I_α^N is defined as the flow of particles out of reservoir α into the quantum dot, while the energy current I_α^E is the total energy current with the same sign convention. In a similar manner, the electrochemical energy current is defined as $\mu_\alpha I_\alpha^N$. Due to the system being at low temperature, we assume that we have no energy transport via phonons. Therefore all energy lost from the electrochemical energy current will turn into heat, i.e. the heat current J_α equals the difference of the total energy current and the electrochemical energy current

$$J_\alpha \equiv I_\alpha^E - \mu_\alpha I_\alpha^N. \quad (7)$$

The main objective for both methods is to derive an expression for the heat flow and electric current through the studied system, and hence examine its thermoelectric properties by studying the relation between these two. The efficiency of the thermoelectric phenomena heat to work conversion is also studied. Each used method is suited for a different regime, and thus using two different methods allows for analysing a wider range of possible situations. The master equation allows the Coulomb interaction to be taken into account, but assumes weak coupling. The scattering theory assumes systems with non-interacting or weakly interacting particles. However, when using this method, the systems can otherwise be complex and have arbitrary coupling.

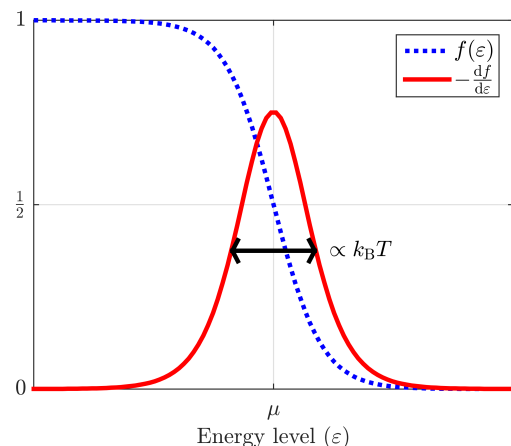


Figure 2: A Fermi function and its derivative. The width of the derivative is proportional to $k_B T$.

2.1 Open Quantum Systems

As mentioned in section 1.2, the quantum dot is connected to its environment in the form of reservoirs. These are in equilibrium, which means that each reservoir α has a fix temperature T_α as well as an electrochemical potential μ_α , also called Fermi energy.

Given that each reservoir contains a large number of fermions, they will follow Fermi-Dirac statistics, described by a Fermi function $f_\alpha(\varepsilon)$ [3]. The reservoirs are in this case solely described by their respective Fermi function. These functions describes the probability of a state at energy ε in the reservoir to be occupied by an electron and is defined as

$$f_\alpha(\varepsilon) \equiv \frac{1}{1 + \exp\left(\frac{\varepsilon - \mu_\alpha}{k_B T_\alpha}\right)}. \quad (8)$$

For compactness we will use the notation $f_\alpha^-(\varepsilon) \equiv 1 - f_\alpha(\varepsilon)$. A example of a Fermi function and its derivative can be seen in figure 2. The Fermi function has the shape of a step function at $T = 0$, and gets flatter for higher temperatures, as seen in equation (8). The width of the derivative is proportional to $k_B T$, which means that it will converge towards a delta function for low temperatures. This is a useful property in calculations where approximations are used, and is therefore worth noticing.

2.2 Master Equation

This method is valid for a quantum dot that is weakly coupled to its environment. The system is described by a Hamiltonian \hat{H} , whose eigenstates are denoted s . These are the different states of the quantum dot, and represent different occupations of its energy levels. The master equation describes the change in the occupation probabilities P_s over time and reads [10]

$$\frac{d}{dt} P_s(t) = \sum_{s'} (W_{ss'} P_{s'}(t) - W_{s's} P_s(t)). \quad (9)$$

$W_{ss'}$ describes a generalized transition rate between a state s' and a state s . Transitions occur due to tunneling of electrons into or out of the system. $W_{ss'}$ is defined as

$$W_{s,s'} = \sum_{\alpha} W_{s,s'}^{\alpha} = \sum_{\alpha} (W_{s,s'}^{\alpha+} + W_{s,s'}^{\alpha-}), \quad (10)$$

where $W_{s,s'}^{\alpha+}$ is the part for electrons tunneling into the quantum dot, while $W_{s,s'}^{\alpha-}$ is the part for electrons tunneling out of the quantum dot into reservoir α . For $s \neq s'$ these elements are given by

$$W_{s,s'}^{\alpha+} = \frac{1}{\hbar} \Gamma_{\alpha} |\langle s | c_1^\dagger | s' \rangle|^2 f_{\alpha}(E_s - E_{s'}) \quad (11)$$

$$W_{s',s}^{\alpha-} = \frac{1}{\hbar} \Gamma_{\alpha} |\langle s | c_1^\dagger | s' \rangle|^2 (1 - f_{\alpha}(E_s - E_{s'})), \quad (12)$$

where Γ_{α} is the coupling strength with respect to reservoir α , c_1^\dagger is the creation operator and E_s is the energy for the system when in state s . These equations can be obtained from Fermi's golden rule. For $s' = s$ the $W_{s,s}$ is given by the Stükelberg condition,

$$W_{s,s}^{\alpha} = - \sum_{s' \neq s} W_{s',s}^{\alpha}. \quad (13)$$

The entire matrix is shown in appendix B.

We consider the system to be in steady state, i.e. $\dot{P}_s(t) = 0$. Then the left hand side of equation (9) is reduced to 0. After solving this homogeneous version of equation (9) for P_s the relations for particle and energy current are given by [10],

$$I_\alpha^N = \sum_{s,s'} (N_{s'} - N_s) W_{s's}^\alpha P_s \quad \text{and} \quad (14)$$

$$I_\alpha^E = \sum_{s,s'} (E_{s'} - E_s) W_{s's}^\alpha P_s, \quad (15)$$

where I_α^N and I_α^E are the electron and energy current respectively.

2.3 Scattering Theory

An alternative method for performing calculations on quantum systems, such as the quantum dot, is scattering theory [8]. This method estimates the currents from incoming and outgoing scattering states in the reservoirs, as illustrated in figure 3. It treats the system as a 'black box' where all properties are incorporated in reflection and transmission properties. This is a powerful tool for describing transport through quantum systems. Here it is particularly important that it allows for treating quantum dot systems with arbitrary coupling strengths. However, interaction between particles inside the system cannot be included in calculations with this method, since it is based on single-particle states in the reservoirs.

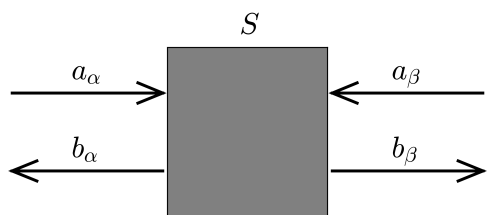


Figure 3: Sketch of the basic idea of scattering theory; a_α, a_β are incoming and b_α, b_β are outgoing scattering states.

The core of the theory is the scattering matrix, whose elements describe the reflection and transmission properties of a given system. In general, the scattering matrix is obtained by relating a vector of the incoming wave functions for all possible states, \vec{a} , to the corresponding vector for transmitted or reflected states, \vec{b} , see figure 3. This relation is written as

$$\vec{b} = S\vec{a}, \quad (16)$$

where the scattering matrix is denoted with S .

The current operator in reservoir α , in terms of the incoming and outgoing scattering states, \hat{I}_α^N is defined as

$$\hat{I}_\alpha^N = \frac{e}{h} \iint e^{-i(E-E')t} [\hat{a}_\alpha^\dagger(E')\hat{a}_\alpha(E) - \hat{b}_\alpha^\dagger(E')\hat{b}_\alpha(E)] dE' dE, \quad (17)$$

where $\hat{a}_\alpha^\dagger, \hat{a}_\alpha, \hat{b}_\alpha^\dagger$ and \hat{b}_α are the creation and annihilation operators for the α -elements of \vec{a} and \vec{b} [11]. \hat{J}_α is obtained by inserting a factor $\frac{E+E'}{2}$ into the integrand. By calculating the expectation value of the current operators for a specific system one gets the particle and heat current expressions

$$I_\alpha^N = -\frac{e}{h} \int \sum_\beta |S_{\alpha\beta}(E)|^2 (f_\beta(E) - f_\alpha(E)) dE, \quad (18)$$

$$J_\alpha = \frac{1}{h} \int (E - \mu_\alpha) \sum_\beta |S_{\alpha\beta}(E)|^2 (f_\beta(E) - f_\alpha(E)) dE, \quad (19)$$

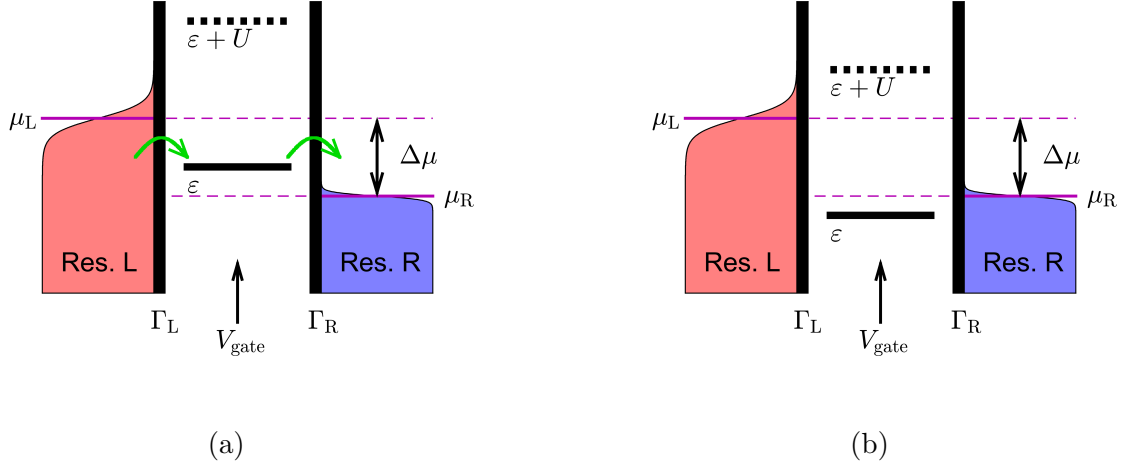


Figure 4: Visualization of a quantum dot with two reservoirs and interacting electrons. In both figures the left reservoir has a higher temperature and higher electrochemical potential than the right reservoir. In (a) the energy level ε is inside the bias window, which allows a current to flow, while in (b) not ε nor $\varepsilon + U$ is inside the bias window which leads to Coulomb blockade.

where $S_{\alpha\beta}(E)$ contains the system properties, while $f_{\alpha/\beta}$ describes the reservoir properties. The integrals corresponds to a sum over all contributing scattering states, each carrying unit flux, and energy $E - \mu_\alpha$. These currents will be used to derive the linear coefficients mentioned in section 1.3.

2.4 Models

The quantum dot can, as mentioned in section 2.2, be described by a Hamiltonian. The most relevant eigenstates of this Hamiltonian describes the occupation of one spin-degenerate energy level, since we normally have only one energy level that contributes to transport. These states are $|0\rangle$, $|\uparrow\rangle$, $|\downarrow\rangle$ and $|2\rangle$, for unoccupied, single spin up and down occupied, and double occupied (one spin up and one spin down) respectively [8]. In this section we present the model used for the quantum dot, and discuss its properties.

2.4.1 General Properties

The occupancy of the different states is affected by the quantum dots connection to adjacent reservoirs. This connection is caused by the overlap between wave functions of electrons in the quantum dot and in the reservoirs, and is described by the coupling strength $\Gamma = \sum_\alpha \Gamma_\alpha$. The size of Γ is typically compared to $k_B T$, and describes the likelihood of electrons tunneling between the dot and the reservoirs, but also the line thickness of the energy level. We consider both strong couplings $\Gamma \gg k_B T$, and weak couplings $\Gamma \ll k_B T$.

Figure 4a shows a sketch of a quantum dot connected to two reservoirs. In section 2.1, we describe how the electron occupancy of the reservoirs is given by a Fermi function, as illustrated by the figure. The likelihood of electron tunneling occurring at an energy depends on the occupancy at that energy. For example, if a reservoir is highly occupied at a certain energy, electrons will tend to tunnel out of that reservoir more than into it, and vice versa for low occupancies. Only electrons which have an energy corresponding to the energy level can tunnel into the dot. In figure 4a this is indicated by a green arrow. Now assume that

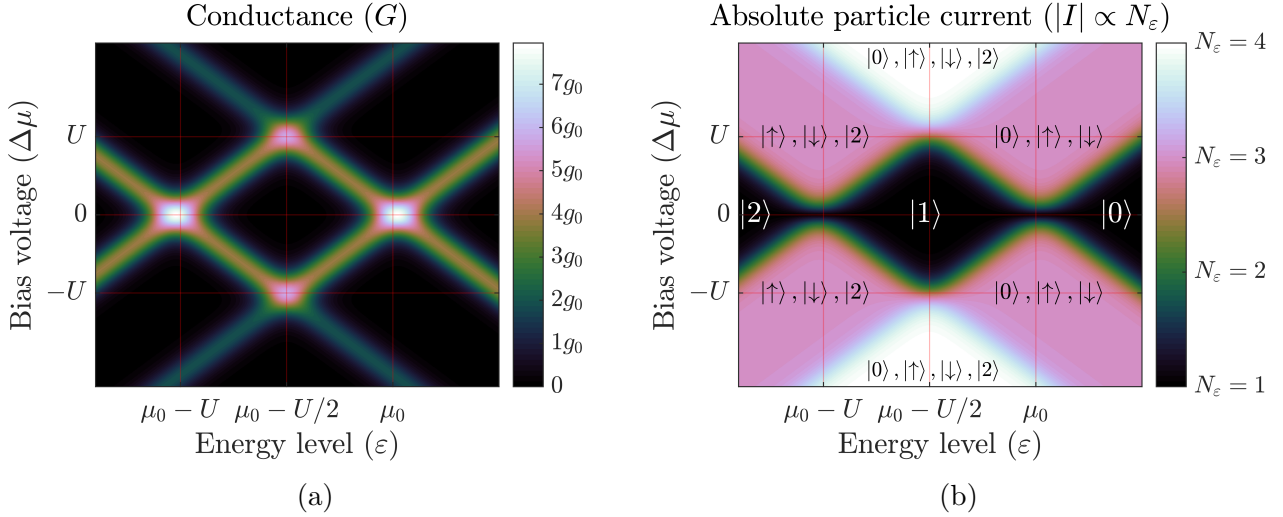


Figure 5: A Coulomb diamond and particle the particle current for a quantum dot with two reservoirs with the electrochemical potentials $\mu_L = \mu_0 + \Delta\mu/2$, $\mu_R = \mu_0 - \Delta\mu/2$, the temperatures $k_B T_L = k_B T_R = 30\Gamma$ and the Coulomb interaction energy $U = 500\Gamma$. In figure 5a we see the conductance, $\partial I/\partial\Delta V$, expressed in $g_0 \equiv e^2(\Gamma_1 + \Gamma_2)/(\hbar\Gamma k_B T)$. In figure 5b we see the absolute particle current, which is proportional to the number of possible states at the same time N_ϵ .

an electron tunnels into the dot and occupies the energy level ϵ . If a second electron would tunnel into the dot, it would have to pay the extra interaction energy U , due to Coulomb interaction between the electrons. This is illustrated with a dashed line in figure 4. Note that in this case, the energy $\epsilon + U$ is located above the reservoirs' Fermi energies μ_α , which means that no tunneling at the present temperature and bias is possible.

When quantum dots with interacting electrons are exposed to a magnetic field, B , the Zeeman effect has to be accounted for. The energy needed for each electron to occupy the energy level is then split into two separate branches, one for each spin. This leads to more complicated behaviour of quantum dot systems, because of more states being available for occupation. In our analysis we mainly stick to the case of $B = 0$, but some results for $B \neq 0$ are presented in appendix A.

2.4.2 Currents and Coulomb Blockade Effect

In order to allow a current between the reservoirs, a bias voltage ΔV or a temperature gradient ΔT has to be applied [8]. In addition, at least one of the energies ϵ or $\epsilon + U$ has to be inside, or at least close to, the bias window $\Delta\mu$. How close depends on the temperature of the reservoir; at higher temperatures the Fermi function becomes stretched out and electrons with energies higher (and lower) than the chemical potential can tunnel into, or out of the dot. An example of current flowing through a quantum dot can be seen in figure 4a. The energy level ϵ is inside the bias window, and the electrons have enough energy to tunnel from the left reservoir into the dot since μ_L is larger than ϵ . Similarly, because μ_R is lower than ϵ , the electron can tunnel out of the dot, and hence a current can flow through it.

Now consider the situation in figure 4b. Here the gate voltage has adjusted the energy level so that it is no longer inside the bias window. Then, if the quantum dot is zero-occupied, one electron can tunnel into it from reservoir L but cannot continue since there are no holes in reservoir R at the energy ϵ . A second electron cannot tunnel into the dot since it would also

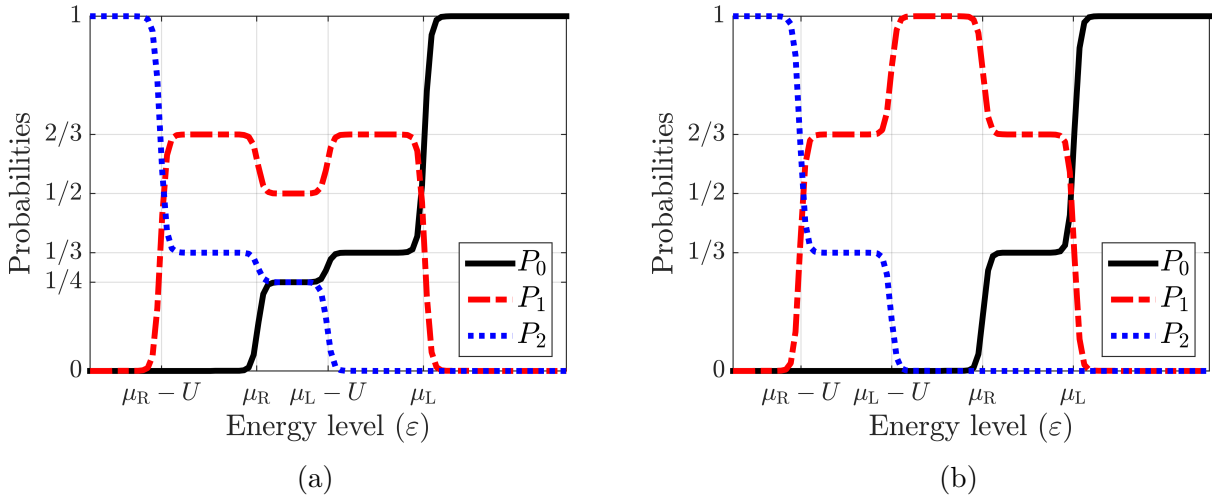


Figure 6: Probabilities for different quantum dot systems. In (a) the bias is greater than the interaction energy, i.e. $\Delta\mu > U$. In contrast in (b) the interaction energy is greater than the bias, i.e. $U > \Delta\mu$.

have to pay the interaction energy U , and reservoir L has no electrons at the energy $\varepsilon + U$. Therefore the quantum dot is stuck in a single state, and now current can flow through it. This blockade effect of the current is known as a Coulomb blockade.

The effect of Coulomb blockade can also be illustrated through a so-called Coulomb diamond [4]. This is a surface plot of the conductance as a function of the bias voltage and gate voltage. An example of a Coulomb diamond can be seen in figure 5a. The black areas represent zero, while the non-black stripes represent finite positive values. Notice that the conductance reaches its maximum when $\Delta\mu = 0$ and $\varepsilon \approx \mu_0 - U$ or $\varepsilon \approx \mu_0$ in figure 5b. This means that either ε or $\varepsilon + U$ is aligned with the chemical potential. We will discuss this in more detail in section 4.3. The black diamond shaped areas in the middle of the plot is due to the Coulomb blockade, i.e. when both ε and $\varepsilon + U$ is outside the bias window. In these regions, a small change in the bias or gate voltage will not result in a change in the current, and thus the conductance is zero. This agrees with figure 5b, which shows the absolute value of the particle current in the $V_{\text{gate}} - \Delta\mu$ plane. There we have a similar black diamond shaped areas corresponding to the quantum dot having just one possible state, either unoccupied ($|0\rangle$), single-occupied ($|1\rangle$) or double-occupied ($|2\rangle$). The single-occupied state can be either $|\downarrow\rangle$ or $|\uparrow\rangle$, but will typically remain in the same state. When there is only one state possible, the current will be zero since the quantum dot has to be able to change states for a current to flow.

Another important aspect of a quantum dot is the occupation probabilities. In figure 6 we see the occupation probabilities for an interacting two-reservoir quantum dot system, for different Coulomb interaction energies U . In both cases the reservoirs have different electrochemical potentials $\mu_L \neq \mu_R$ but the same temperature $T_L = T_R$. The difference between the cases is that in figure 6a the bias is greater than the interaction energy, which allows both energies ε and $\varepsilon + U$ to be inside the bias window at the same time. Since the particle current is proportional to the amount of states the system can be in at the same time, this figure is approximately a cross section of figure 5b for $\Delta\mu > U$. On the contrary, in figure 6b the bias is smaller than the interaction energy, in this case only one of the energies can be inside the bias window at the time. The probability graphs in figure 6 is approximately a cross section of figure 5b along a constant $\Delta\mu$.

2.4.3 Modeling a Quantum Dot Using a Double Delta Barrier

In order to calculate the transmission with scattering theory the quantum dot is approximated with a double delta barrier with the coupling strengths Γ_L and Γ_R . See figure 7 for an illustration of electrons scattered at the double barrier. Then the scattering matrix is unitary and can be written

$$S = \begin{bmatrix} r & \bar{t} \\ t & \bar{r} \end{bmatrix}, \quad (20)$$

where r and t are the reflection and transmission coefficients and \bar{r}, \bar{t} their complex conjugates [8]. For a two-reservoir system we set $\alpha = L$, $\beta = R$ and $\sum_{\beta} |S_{\alpha\beta}(E)|^2 = T(E)$ in equation (18) and (19), where $T(E) \equiv |t(E)|^2$ is the transmission at energy E . If the resonance energy for the double delta barrier is E_{res} and the coupling strengths are Γ_L and Γ_R the transmission can be approximated as

$$T(E) = \frac{\Gamma_L \Gamma_R}{(E - E_{\text{res}})^2 + \frac{1}{4}(\Gamma_L + \Gamma_R)^2}. \quad (21)$$

When studying systems of n energy levels (resonance energies), the transmission becomes a sum of transmissions on a form similar to equation (21). The general expression for transmission can then be written as

$$T_{\alpha\beta}(E) = \sum_{i=1}^n \frac{\Gamma_{\alpha} \Gamma_{\beta}}{(E - E_{\text{res}}^{(i)})^2 + \frac{1}{4}\Gamma^2}, \quad (22)$$

where the resonance energy for energy level i is denoted as $E_{\text{res}}^{(i)}$ and $\Gamma = \sum_{\alpha} \Gamma_{\alpha}$.

3 Thermoelectric Properties in the Linear Regime

In this chapter, thermoelectric properties in the linear regime are presented, valid for small ΔT and ΔV on the scale of Γ . We investigate the effects that different coupling strengths and Coulomb interaction between electrons in the quantum dot have on the presented linear coefficients. The linear coefficients are then used to derive an expression for the Seebeck coefficient, which reveals the thermoelectric properties of the studied systems. In addition, an efficiency based on the linear Onsager coefficients is calculated.

3.1 Single Energy Level with Spinless Particles

First we examine a simple case with spinless particles. The system used is a single energy-level quantum dot connected to two reservoirs and a gate, similar to figure 4, with the only difference being that we only consider spinless particles. For weak coupling, i.e. $k_B T \gg \Gamma$, the linear response coefficients become

$$\begin{aligned} G &= -\frac{e^2}{\hbar} \frac{\Gamma_L \Gamma_R}{\Gamma} \left(\frac{\partial f}{\partial \varepsilon} \right), & L &= -\frac{e}{\hbar T_0} \frac{\Gamma_L \Gamma_R}{\Gamma} \left(\frac{\partial f}{\partial \varepsilon} \right) (\varepsilon - \mu_0), \\ M &= -\frac{e}{\hbar} \frac{\Gamma_L \Gamma_R}{\Gamma} \left(\frac{\partial f}{\partial \varepsilon} \right) (\varepsilon - \mu_0), & \Theta &= -\frac{1}{\hbar T_0} \frac{\Gamma_L \Gamma_R}{\Gamma} \left(\frac{\partial f}{\partial \varepsilon} \right) (\varepsilon - \mu_0)^2. \end{aligned} \quad (23)$$

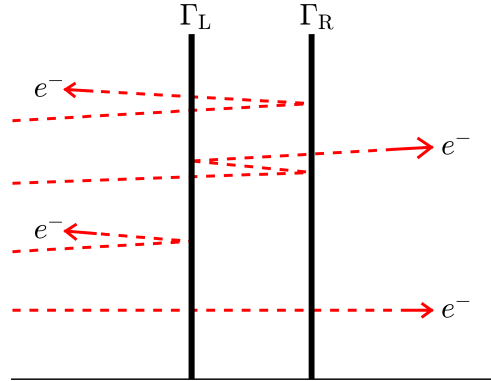


Figure 7: Electrons scattered at a double delta barrier.

These expressions help to get an intuitive understanding of how transport through a weakly coupled quantum dot is carried out. The coefficients L and M are proportional to $\varepsilon - \mu_0$, which is the amount of heat that an electron with energy ε carries when leaving or entering a reservoir at potential μ_0 . This quantity can be both positive and negative, depending on ε , so we can have heat transport either with or against the direction of the particle current. Furthermore, when $\varepsilon = \mu_0$, there can be no heat transport. The driver of electronic transport is the bias, ΔV and ΔT , as described by the Onsager matrix in equation (1). The coefficients G, L, M and Θ each describe a different type of transport, listed in section 1.3, and tell us how the respective transport depends on the corresponding bias. As seen in equation (23), all the coefficients are proportional to $\frac{\Gamma_R \Gamma_L}{\Gamma} \left(\frac{\partial f}{\partial \varepsilon} \right)$, which describes the scale of the interaction between the reservoirs and the dot. Since the width of $\frac{\partial f}{\partial \varepsilon}$ is proportional to $\frac{1}{k_B T_0}$, so are the widths of the coefficients. This explains why the quantum dot requires very low temperatures in order to exhibit its characteristic properties; for large $k_B T_0$, $\frac{\partial f}{\partial \varepsilon}$ is widened to a point where it is almost constant with respect to ε , and the system properties will no longer depend on the position of the energy level. At high temperatures, the Fermi levels in the reservoirs are not distinct, and there are electrons and holes available in a large range of energies.

Here we have a Seebeck coefficient that is linear in $\varepsilon - \mu_0$, given by

$$S = \frac{\varepsilon - \mu_0}{eT_0}. \quad (24)$$

The Seebeck coefficient describes the potential difference induced by a temperature gradient, in units of volts per kelvin. Here we see that the Seebeck effect can be modulated by changing the system temperature or ε . We stated in section 1.3 that S can be interpreted as the average energy per unit charge transferred at the temperature T_0 . This holds up in the light of equation (24), since $\Delta\mu \approx 0$ so there will be no transfer of electrochemical energy. The only energy that is transferred will be heat, and as before the heat transferred per unit charge is $\varepsilon - \mu_0$.

The Fourier heat coefficient, K , is zero for this system. As previously mentioned, it describes heat flow without charge current, which is apparently impossible in this system. This is explained by the assumption of weak coupling, $\Gamma \ll k_B T_0$, and thereby that we only have electron tunneling at a single energy ε . The only way that K can become non-zero is if there is zero total charge current, due to currents with opposite direction but the same size, that carries more heat in one direction than the other. However, here all electrons that tunnel carry the same heat, $\varepsilon - \mu_0$, meaning that there will never be a net heat transfer without a non-zero charge current.

As discussed in section 1.4, the quantum dot can work as a heat engine. The setup where this is done is detailed in figure 10a. Worth noting is that the hot reservoir also has the higher μ , but despite this the particle current is moving against the bias. Heat is transferred from the hot reservoir to the cold, while performing electrical work by moving electrons from the cold reservoir to the hot reservoir. The efficiency η , given by equation (6), then becomes

$$\eta = -\frac{\Delta\mu}{\varepsilon - \mu_0}. \quad (25)$$

Since this is an approximation for small ΔV and ΔT , high efficiency can only be obtained by a small $\varepsilon - \mu_0$. However, the heat flow through the system is proportional to $\varepsilon - \mu_0$, and thus increasing the efficiency leads to a process with lower power. A more extensive discussion of the upper limit of the efficiency is provided in section 4.2.1. It is important to note however that while this expression might seem to provide values both negative and larger than one for some values of ε , this occurs in a region where the quantum dot is not converting heat to work and η is thus not defined in these regimes.

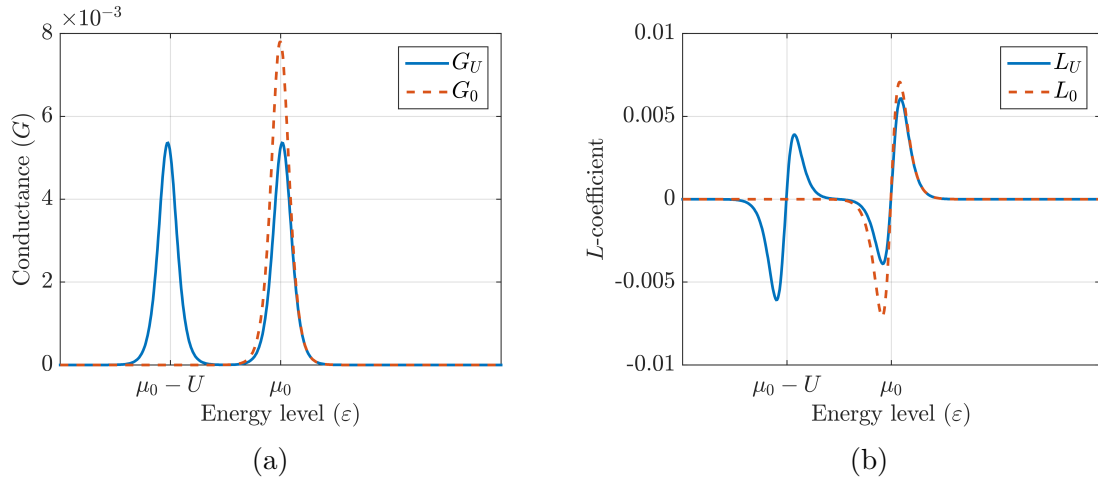


Figure 8: Conductance G and L -coefficient as functions of the position of the energy level ε , for both an interacting two-reservoir system (G_U, L_U) and a non-interacting two-reservoir system (G_0, L_0).

3.2 Single Energy Level with Interacting Electrons

Let us now consider the effects of Coulomb interaction on the thermoelectric properties. Here we use the same system as in the previous section, but with electrons with spin instead of spinless electrons. In our single energy level there is now room for two electrons with different spin, but to add the second electron the extra energy U is required due to the Coulomb interaction. In this system we can no longer only transfer electrons with energy ε through the system, but also electrons with energy $\varepsilon + U$. This makes the linear transport coefficients more complicated, so we introduce a couple of notations:

$$f \equiv f(\varepsilon), \quad f_U \equiv f(\varepsilon + U), \quad \sigma \equiv \frac{2}{k_B T_0} \frac{\Gamma_R \Gamma_L}{\Gamma} \frac{f f_U^-}{f + f_U^-}. \quad (26)$$

With these abbreviations the linear coefficients become

$$\begin{aligned} G &= \frac{e^2 \sigma}{\hbar} (f^- + f_U), & L &= \frac{\sigma e}{\hbar T_0} [(\varepsilon - \mu_0) f^- + (\varepsilon + U - \mu_0) f_U], \\ M &= \frac{\sigma e}{\hbar} [(\varepsilon - \mu_0) f^- + (\varepsilon + U - \mu_0) f_U], & \Theta &= \frac{\sigma}{\hbar T_0} [(\varepsilon - \mu_0)^2 f^- + (\varepsilon + U - \mu_0)^2 f_U]. \end{aligned} \quad (27)$$

By setting $U = 0$ these coefficients simplify to equation (23), as one would expect. This means that the most transport for a given Γ is obtained when $\Gamma_L = \Gamma_R$. The main effect of the Coulomb interaction on the conductance G is that it now has two peaks instead of one, with the distance U between them. The effect on the other coefficients is similar, in that it adds a second set of the same features. A comparison of G and L for $U = 0$ and $U \neq 0$ can be found in figure 8.

The Fourier heat coefficient, $K = \Theta - \frac{LM}{G}$, exhibits an interesting behaviour in this system. In section 1.2, we mentioned that K represents heat flow without charge current, and in section 3.1 we showed that $K = 0$ for $U = 0$. However, in this case K is non-zero in a region between $\varepsilon = \mu_0$ and $\varepsilon + U = \mu_0$, as shown in figure 9a. This has some interesting implications. In this system electrons can travel through the quantum dot at two discrete energies, with an average direction described by the difference between Fermi functions of the two reservoirs. For some situations, this difference can, however, take different signs at ε and $\varepsilon + U$, meaning that the particle currents on the two energies will take different directions. The two currents can have opposite directions but equal sizes, which leads to a total current

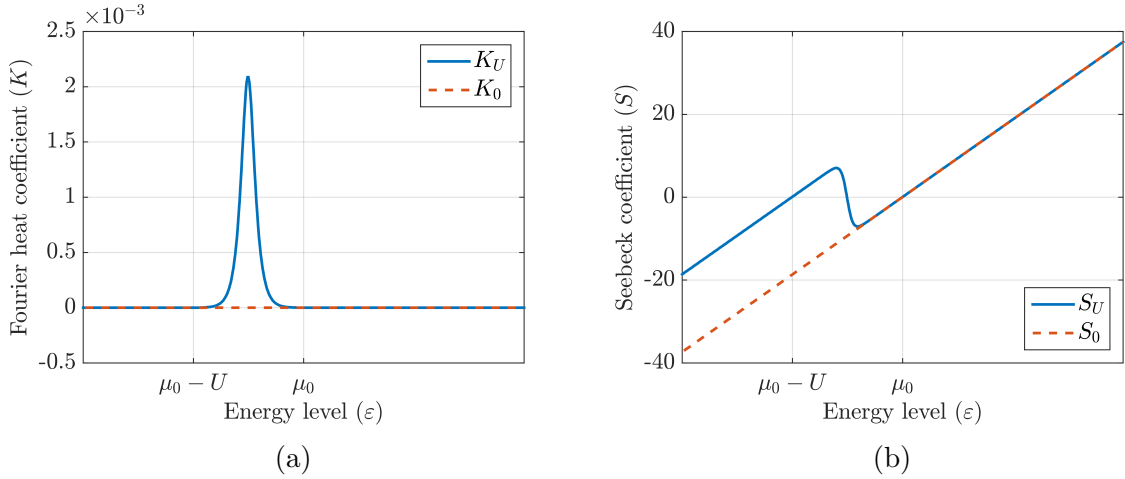


Figure 9: Fourier heat coefficient K and Seebeck coefficient S as functions of the position of the energy level ε , both in the case of an interacting two-reservoir system (K_U, S_U) and a non-interacting two-reservoir system (K_0, S_0).

$I = 0$. For particle transport on a single energy, this would inevitably lead to $J = 0$. However, here the particles can carry different amounts of heat. The electrons traveling on the lower energy carry a heat of $\varepsilon - \mu_0$, while those on the upper energy carry a heat of $\varepsilon + U - \mu_0$. So, for every couple of electrons that exchange places, heat equal to the Coulomb interaction energy U is transferred. For this system we have a Seebeck coefficient given by

$$S = \frac{L}{G} = \frac{1}{eT_0} \left[\varepsilon - \mu_0 + \frac{U f_U}{f^- + f_U} \right]. \quad (28)$$

Apparently the first term is exactly the same as in the non-interacting case, see equation (24). The second term then is due to the Coulomb interaction, and gives rise to the non-linearity seen in figure 9b. This deviation is located in the same region where $K \neq 0$, for ε between μ_0 and $\mu_0 - U$. A closer look at equation (28) reveals that when ε is located far below μ_0 , so that $f(\varepsilon) \approx 1$, the Seebeck coefficient becomes

$$S = \frac{\varepsilon + U - \mu_0}{eT_0}. \quad (29)$$

This is when most of the electron tunneling occurs on energy $\varepsilon + U$, and is consistent with the interpretation of S as average energy carried per particle. The region where S has a negative slope, as discussed earlier, is where transport is occurring both on energy ε and $\varepsilon + U$. From equation (29) we can also see that the distance between the two intersections with the x -axis is U , and that the distance in y -direction between the Seebeck coefficients in equations (24) and (29) is $\frac{U}{eT_0}$.

The efficiency for this system becomes

$$\eta = -\frac{\Delta\mu}{\varepsilon - \mu_0} - \frac{U f_U \Delta\mu}{(\varepsilon - \mu_0)((\varepsilon - \mu_0)f^- + (\varepsilon + U - \mu_0)f_U)}. \quad (30)$$

Similar to the Seebeck coefficient, the efficiency consists of two terms; one which is equivalent to the η in the non-interacting case in equation (25), and another which takes the interaction energy U into account. In a situation similar to the one showed in figure 10a, and discussed in section 3.1, this second term would have a negative impact on the efficiency. This is due to the same effect that causes K to be non-zero, namely counterflowing currents causing heat flow without charge current. This heat flow cannot be converted to work, and will thus lower the efficiency of the process.

3.3 Non-interacting System and Strong Coupling

Finally we investigate a strongly coupled system, $k_B T \ll \Gamma$. To do this we use the scattering integrals from equations (18) and (19). This allows us to obtain linear response coefficients that are valid for any number of reservoirs and energy levels, as long as the transmission for the given situation is known. These coefficients are

$$\begin{aligned} G &= \frac{e^2}{h} T(\mu_0), & L &= \frac{e\pi^2 k_B^2 T_0}{3h} \left. \frac{\partial T}{\partial E} \right|_{\mu_0}, \\ M &= \frac{e\pi^2 k_B^2}{3h} \left. \frac{\partial T}{\partial E} \right|_{\mu_0}, & \Theta &= \frac{\pi^2 k_B^2 T_0}{3h} T(\mu_0). \end{aligned} \quad (31)$$

The coefficients are dependent on the transmission T at the Fermi energy μ_0 . To model the quantum dot we use a Lorentzian shape for T , as described by equation (21), and a sum of Lorentzians for more than one energy level. The resonance energy E_{res} represents the position of the energy level, so for $T(\mu_0)$ E_{res} becomes $\varepsilon - \mu_0$. If ε is close to the Fermi energy, the dependence of Γ is linear in all the coefficients, similar to the case of weak coupling. However, if $\varepsilon - \mu_0$ is large, then the dependence is quadratic, $T \propto \Gamma_L \Gamma_R$. Of course, in this region there is almost no transport in the considered systems.

By using the transmission for a single resonance and two reservoirs, i.e. equation (21), the Seebeck coefficient becomes

$$S = \frac{\pi^2 k_B^2 T_0}{3e} \frac{2(\varepsilon - \mu_0)}{(\varepsilon - \mu_0)^2 + \frac{1}{4}\Gamma^2}. \quad (32)$$

In some respects this is very different from the case of weak coupling, see equation (24). However, if $(\varepsilon - \mu_0) \ll \Gamma$, which is reasonable since this is the region of strong coupling, S becomes linear in ε . Perhaps the most noteworthy irregularity is the difference in temperature dependence. For weak coupling, $S \propto \frac{1}{T_0}$, but for strong coupling, $S \propto T_0$.

With scattering theory we can illustrate the interpretation of S as an average energy by looking at the origin of L and G . The linear coefficients are derived from the scattering integrals for I and J . With the approximations used earlier for linear response, we receive for the Seebeck coefficient

$$S = \frac{1}{T_0} \frac{\int (E - \mu_0) T(E) [f_L(E) - f_R(E)] dE}{\int T(E) [f_L(E) - f_R(E)] dE}. \quad (33)$$

This looks like an average, or expectation value, of the energy $(E - \mu)$ with respect to the distribution $T(E)(f_L(E) - f_R(E))$. Since this distribution describes the amount of particle transfer for each energy, equation (33) becomes the average energy transferred particle, weighted by transfer amount for that energy.

The Fourier heat coefficient, $K = \Theta - \frac{LM}{G}$, becomes non-zero in this system. This is because of the assumption of large Γ , which implies that the energy level is subject to line widening. For the same reasons as in the previous section, it is now possible to have counterflowing currents at different energies, which cause a non-zero heat flow. As before, $K \neq 0$ negatively affects the efficiency of heat to work conversion. In conclusion, strong coupling allows for larger currents i.e. more power, however lowers the efficiency of power production.

4 Thermoelectric Properties in the Non-Linear Regime

In this section we consider the case of arbitrary ΔT and ΔV , but weak coupling, i.e. $\Gamma \ll k_B T$. The reason for limiting the analysis to the regime of weak coupling is that equations (18)

and (19) are treatable with the master equation under this assumption. This analysis can be extended to general coupling strengths if equations (18) and (19) are treated with numerical methods, which is not done here. Instead, this section is limited to weak coupling expressions for particle and heat currents are derived using probabilities given by the master equation.

4.1 Single Energy Level with Spinless Electrons

For a single-level quantum dot adjoining an arbitrary amount of reservoirs, we start by considering the case of spinless electrons. The occupation probabilities in this case become

$$P_0 = \frac{1}{\Gamma} \sum_{\alpha} \Gamma_{\alpha} f_{\alpha}^{-} \quad \text{and} \quad P_1 = \frac{1}{\Gamma} \sum_{\alpha} \Gamma_{\alpha} f_{\alpha}, \quad (34)$$

and the particle current becomes

$$I_{\alpha}^N = \frac{1}{\hbar} \frac{\Gamma_{\alpha}}{\Gamma} \sum_{\beta \neq \alpha} \Gamma_{\beta} (f_{\alpha} - f_{\beta}). \quad (35)$$

By definition of the energy current and heat current we obtain

$$I_{\alpha}^E = \varepsilon I_{\alpha}^N \quad \text{and} \quad J_{\alpha} = (\varepsilon - \mu_{\alpha}) I_{\alpha}^N. \quad (36)$$

This shows that the heat transport for a non-zero particle current is proportional to the energy difference between the energy level and the electrochemical potential of the studied reservoir. A non-zero heat current is only possible when the energy level and the electrochemical potential does not align with each other. This is true for a arbitrary setup of electrochemical potentials, and hence also in the large bias regime. Moreover, this result shows that the heat transported in a given quantum dot system is solely determined by the energy of each individual particle.

4.2 Heat to Work Conversion

It is interesting to study the possibility to extract work from heat. To be able carry out these studies, the measure for system produced power, P , is needed. For this analysis, consider a single-energy level, non-interacting, system connected to two reservoirs denoted cold and hot respectively. Two systems of this kind are shown in figures 10a and 10b. As can be seen in these figures, there are three possible regimes for the energy level to be in. When located under $\varepsilon_{\text{Carnot}}$, the system performs heat to work conversion, when located between $\varepsilon_{\text{Carnot}}$ and $\varepsilon_{\text{cool}}$, heat is moved from the colder reservoir to the warmer, and for energies above $\varepsilon_{\text{cool}}$ the system produces heat from work. As we are interested in the ability to convert heat into work, let us consider the regime where ε is lower than $\varepsilon_{\text{Carnot}}$. The work converted from heat is then given by

$$P = J_{\text{H}} + J_{\text{C}}, \quad (37)$$

where J_{H} and J_{C} denote the heat flow out of the reservoirs. Due to the fact that we are studying a two reservoir system, particle conservation gives us that $I_{\text{H}}^N = -I_{\text{C}}^N$. Using the general definitions of these heat currents and setting $U = 0$ leaves us with a power given by

$$P = (\varepsilon - \mu_{\text{H}}) I_{\text{H}} + (\varepsilon - \mu_{\text{C}}) I_{\text{C}} = \frac{\Gamma_{\text{H}} \Gamma_{\text{C}}}{\Gamma} \frac{\mu_{\text{C}} - \mu_{\text{H}}}{\hbar} (f_{\text{H}} - f_{\text{C}}). \quad (38)$$

Each of the two Fermi functions is a function of the energy level ε as well as the reservoir parameters μ and T . Thus, the total power depends on the parameters ε, μ, T and Γ of both

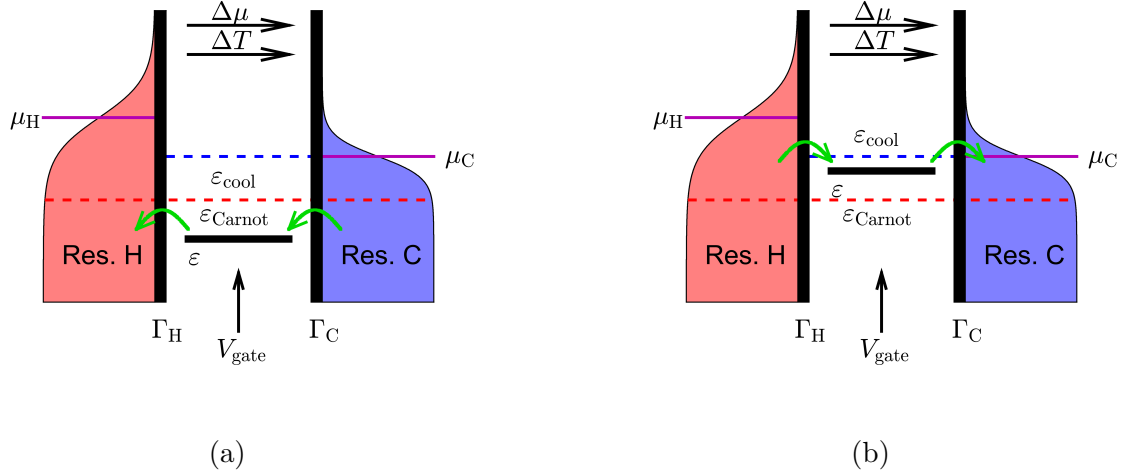


Figure 10: A quantum dot with two reservoirs which have a temperature gradient, $T_H > T_C$ and an electrochemical gradient $\mu_H > \mu_C$. In (a) we have $\varepsilon < \varepsilon_{\text{Carnot}}$ which leads to heat to work conversion. In (b) we have ε between $\varepsilon_{\text{Carnot}}$ and $\varepsilon_{\text{cool}}$, which leads to cooling of the colder reservoir.

the cold and hot reservoir. In order to understand how these parameters influence the change in P , it is sensible to differentiate with respect to them. The desirable case would be to find a maximum. In order to obtain this, the derivatives with respect to all the parameters would have to be equal to 0 at the same time. By differentiating with respect to them we find that in order to have a non-zero power output, the condition for an extrema is

$$\frac{\partial P}{\partial \varepsilon} = \frac{\partial P}{\partial \mu_H} = \frac{\partial P}{\partial \mu_C} = 0 \quad \text{when} \quad \frac{\partial f_H}{\partial \varepsilon} = \frac{\partial f_C}{\partial \varepsilon}. \quad (39)$$

In conclusion; to be able to convert the maximum amount of heat into work, two terminal systems should therefore be designed in such a way that the Fermi functions fulfill equation (39). An important note, however, is to also check that the used properties yield a maximum and not a minimum, as both are possible outcomes from using this equation.

4.2.1 Efficiency of the Conversion

A system's potential for heat to work conversion is however not only dependent on the total heat that can be extracted, but also on how effective this transfer can be. In the two reservoir case, the energy source is the hot reservoir, and thus a logical definition of efficiency is

$$\eta \equiv \frac{P}{J_H} = 1 - \frac{\varepsilon - \mu_C}{\varepsilon - \mu_H}. \quad (40)$$

This can be proven to have an upper limit defined by the Carnot efficiency, as expected. To do this, let us study the point where the efficiency of heat to work conversion would be maximized. To have heat to work conversion, in the first place, the sign of P would have to be non-negative. In the case of a negative sign, it would no longer be heat to work conversion, and is hence of no interest in this analysis. As seen in equation (38), the sign of P depends on the difference between the Fermi functions, i.e. $f_H - f_C$. Maximum efficiency will be obtained when there is no heat to work conversion at all, and hence the energy of maximum efficiency, $\varepsilon_{\text{Carnot}}$, is obtained in the point where the Fermi functions align, $f_H = f_C$. This

is schematically shown in figure 10. The restriction that $\varepsilon_{\text{Carnot}}$ is placed in such a way that $f_{\text{H}} = f_{\text{C}}$ yields

$$\frac{\varepsilon_{\text{Carnot}} - \mu_{\text{H}}}{T_{\text{H}}} = \frac{\varepsilon_{\text{Carnot}} - \mu_{\text{C}}}{T_{\text{C}}} \Leftrightarrow \varepsilon_{\text{Carnot}} = \frac{\mu_{\text{H}}T_{\text{C}} - \mu_{\text{C}}T_{\text{H}}}{T_{\text{C}} - T_{\text{H}}}. \quad (41)$$

When plugged into equation (40), this gives an efficiency $\eta = \eta_{\text{Carnot}} \equiv 1 - \frac{T_{\text{C}}}{T_{\text{H}}}$, and hence the efficiency is bounded by the classical Carnot efficiency.

4.2.2 Maximize Power or Efficiency

In conclusion, section 4.2 and section 4.2.1 tells us that heat to work conversion is limited by two factors, namely power production and efficiency. However, these two quantities are heavily correlated, and maximizing the efficiency was in section 4.2.1 shown to reduce the available power to zero. Because of this, there is no general answer to what the optimal combination of efficiency and power production is, as it is system dependent.

For example; a system with limited power supply would benefit from a high conversion efficiency, as the amount of 'wasted' energy then would be minimal. In many applications, power supply is not a problem. In these cases, it is often more relevant to look at the property efficiency at maximum power, η_{MP} . As the name suggests, this is a measure of how efficient the heat to work conversion is when the maximum amount of work is produced. A relation between power output and efficiency is shown in figure 11. It is clear from this that the efficiency at maximum power is different from the maximum efficiency, η_{Carnot} .

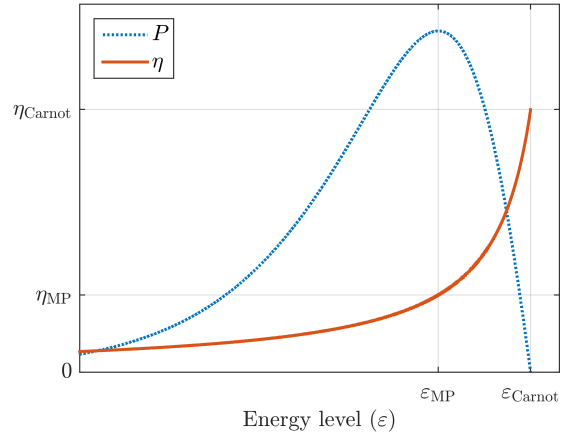


Figure 11: Produced power P and the efficiency η . The system reaches its maximum power with the efficiency η_{MP} output when $\varepsilon = \varepsilon_{\text{MP}}$. It reaches the Carnot efficiency η_{Carnot} when $\varepsilon = \varepsilon_{\text{Carnot}}$. Note that the power output at the Carnot efficiency is zero.

4.3 Spin Degenerate Energy Level with Interacting Electrons

Now let us consider a system similar to the one in section 4.1, with the only difference being that we now have electrons with spin. This means that due to the Pauli principle, it is possible for two electrons to occupy the energy level at the same time as long as they have different spin.

To increase readability, we introduce the following definitions,

$$\begin{aligned} f_{\alpha} &= f_{\alpha}(\varepsilon), & f_{U\alpha} &= f_{\alpha}(\varepsilon + U), \\ f_{\Sigma} &= \sum_{\alpha} \Gamma_{\alpha} f_{\alpha}, & f_{U\Sigma} &= \sum_{\alpha} \Gamma_{\alpha} f_{U\alpha}. \end{aligned} \quad (42)$$

With these definitions we get the particle current

$$I_{\text{L}}^{\text{N}} = \frac{2\Gamma_{\text{L}}\Gamma_{\text{R}}}{\hbar} \frac{f_{\text{L}} - f_{\text{R}} + f_{\text{R}}f_{U\text{L}} - f_{\text{L}}f_{U\text{R}}}{f_{\Sigma} + f_{U\Sigma}}, \quad (43)$$

where indices L and R refer to the left and right hand side reservoir respectively. This particle current yields a heat flow of the form

$$J_L = -\frac{2\Gamma_L\Gamma_R}{\hbar\Gamma} \frac{(\varepsilon - \mu_L)f_{U\Sigma}^-(f_L - f_R) + (\varepsilon + U - \mu_L)f_\Sigma(f_{UL} - f_{UR})}{f_\Sigma^- + f_{U\Sigma}^-}. \quad (44)$$

One key difference between the currents in equations (43) and (44) with the ones in section 4.1, is that it is now possible to have a heat current without a charge current. An example of this is illustrated in figure 12. In this situation, each electron heats and cools the colder and the warmer reservoir respectively with $U/2$, i.e. the warmer reservoir transfers heat to the colder reservoir. Since an equal amount of electrons tunnel in both directions, the net particle current is zero.

5 Charge and Heat Separation

For some thermoelectrical setups, it might be desirable to have charge and heat currents splitting up into different parts of the system. In this section we consider a three-terminal system like the one in figure 13. The goal is to have charge current and heat flow going out of one reservoir, and then have the charge current go into the second terminal while the third is heated. Whether this is possible or not is investigated in this section.

5.1 Spinless Particles

For the system with spinless particles, and tunneling on a single energy ε , the heat flow J_α out of reservoir α is always directly proportional to the particle current out of that reservoir, as per equation (36). Since the heat flow is tied to the particle current it is impossible to completely separate charge and heat in this system.

5.2 Coulomb Interacting Electrons

In section 3.2 we showed that in the Coulomb interacting system the Fourier heat coefficient can be non-zero. This means that it is possible to have a heat flow without a particle current. In the three-terminal setup, we will use one of the terminals as a voltage probe, see figure 13. The voltage probe has infinitely high resistance and is therefore described by the condition $I_{\text{probe}} = 0$. In the linear regime, the current out of a reservoir in a three terminal system is given by

$$I_1 = G_{12}\Delta V_{12} + L_{12}\Delta T_{12} + G_{13}\Delta V_{13} + L_{13}\Delta T_{13}. \quad (45)$$

If we for example set $I_{\text{probe}} \equiv I_2 = 0$, then having $J_2 \neq 0$ would require thermoelectric effects in the transport between reservoirs 1 and 3. Since M is proportional to L , $L = 0$ tells us that

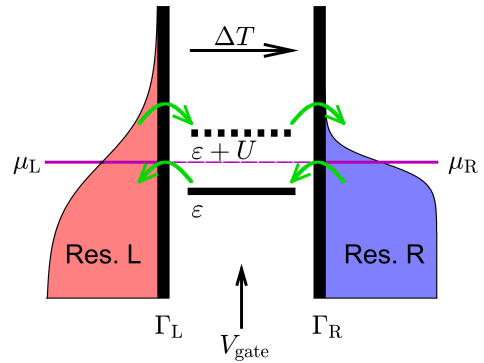


Figure 12: A weakly coupled interacting quantum dot without a bias, $\Delta\mu = 0$, but a temperature gradient, $\Delta T > 0$. ε is at $\mu_0 - U/2$ and $\varepsilon + U$ at $\mu_0 + U/2$. The particle currents cancel out but the electrons still carry heat from the warmer reservoir to the cooler.

there is no thermoelectric effect present. Applying the probe condition, we find after some calculation that

$$\begin{aligned} L_{13} &= \frac{L_{12}G_{21} + L_{12}G_{23} - L_{21}G_{12} - L_{23}G_{12}}{G_{32} + G_{32}} \\ L_{31} &= \frac{L_{32}G_{21} + L_{21}G_{32} - L_{32}G_{23} - L_{32}G_{23}}{G_{32} + G_{32}}. \end{aligned} \quad (46)$$

Apparently the condition for having $I_2 = 0$ while $J_2 \neq 0$, i.e. $L_{13} \neq 0$ and $L_{31} \neq 0$, is $G_{\alpha\beta}L_{\beta\alpha} \neq G_{\beta\alpha}L_{\alpha\beta}$. While the linear coefficients describing this situation have not been presented explicitly, they are similar to equation (27) but with $\Gamma = \Gamma_1 + \Gamma_2 + \Gamma_3$. Note however that these coefficients were derived under the assumption of energy independent couplings, and thus will always fulfil $G_{\alpha\beta}L_{\beta\alpha} = G_{\beta\alpha}L_{\alpha\beta}$.

From this we see that the only thing that could cause an asymmetry in the coefficients would be the coupling. However it is not enough to have an asymmetric coupling $\Gamma_1 \neq \Gamma_3$, which would still lead to symmetric Onsager coefficients, since they would still be given by the same expressions. The couplings would have to be asymmetrically energy dependent, i.e.

$$\frac{\partial\Gamma_1}{\partial\varepsilon} \neq A \frac{\partial\Gamma_3}{\partial\varepsilon}, \quad (47)$$

for any constant A . If this is the case we can have $L_{13} \neq 0$, $L_{31} \neq 0$, which would allow for separation of heat and charge, in the sense that $I_2 = 0$ while $J_2 \neq 0$.

6 Conclusions

In this project, we have studied the ability of a quantum dot to act as a heat engine, or a heat pump, i.e. convert heat to work or extract heat from a cold reservoir. This was done by investigating the effects of different system characteristics on the thermoelectric properties of the system. Below we provide a brief summary of the results, as well as some discussion on possible applications.

For a quantum dot with a single non-spin degenerate energy level in a weakly coupled system, we have found that the heat flow J_α for each reservoir α is proportional to its particle flow I_α^N . This means that for this kind of system, there cannot be a heat flow without a particle current. We have studied the efficiency of heat to work conversion, and found that its upper limit is the Carnot efficiency when considering non-linear effects, but it is only reached in a zero power output process. The difference between the Carnot efficiency and the efficiency at maximum power depends on the reservoirs' characteristics.

In contrast, for a quantum dot with a spin degenerate energy level in a weakly coupled system, we have found that the particle current and heat flow depends on the interaction energy U between the electrons in the system, since the Coulomb interaction is a means to store energy in the dot. In this system, counterflowing charge currents can lead to a heat flow

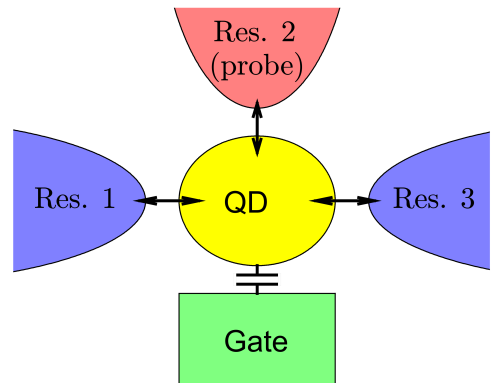


Figure 13: Quantum Dot with three reservoirs, where reservoir 2 is a voltage probe.

without a charge current. This negatively impacts the efficiency of heat to work conversion, since this heat flow cannot be converted to work.

For a system with an interacting quantum dot connected to two reservoirs and a voltage probe, we have shown that with asymmetrically energy dependent coupling strengths we can separate heat flow and charge current. This means that while doing electric work between the reservoirs due to a voltage gradient, the heat for this process is extracted from the probe. However, we also have shown that this process is not possible with symmetrically energy dependent coupling strengths.

For a strongly coupled non-interacting system in the linear regime, the Fourier heat was shown to be non-zero. This means that heat can flow without a charge current, which negatively affects the efficiency in a process of heat to work conversion.

It is important to note that the quantum dot operates in very low temperatures. That being said, there still seems to be potential for several useful applications of this kind of system. We have shown how a quantum dot connected to two or more reservoirs can be used for cooling, converting heat to work, selectively eliminating temperature and voltage gradients, and separating heat flow from charge current. All of these processes could have uses in low-temperature microscopic circuitry, but would require further investigation.

References

- [1] S. B. Desai, S. R. Madhupathy, A. B. Sachid, J. P. Llinas, Q. Wang, G. H. Ahn, G. Pitner, M. J. Kim, J. Bokor, C. Hu, H.-S. P. Wong, and A. Javey, “MoS₂ transistors with 1-nanometer gate lengths”, *Science*, no. 354, pp. 99–102, Oct. 2016.
- [2] J. Vanherck, “Time-dependent particle and energy currents through interacting quantum dots”, 88, Master’s thesis, 2016.
- [3] S. Jürgens, “Thermoelectric performance of quantum dots driven by time-dependent fields”, Fakultät für Mathematik, Informatik und Naturwissenschaften der RWTH Aachen, 2012.
- [4] T. Ihn, *Semiconductor Nanostructures*. Oxford University Press, 2010.
- [5] J. Was, *Fundamentals of Nanoelectronics, Single-electron devices*, S. Blügel, M. Luysberg, K. Urban, and R. Waser, Eds. Forschungszentrum, Zentralbibliothek, 2003, ISBN: 389336319X.
- [6] C. Volk, S. Engels, C. Neumann, and C. Stampfer, “Back action of graphene charge detectors on graphene and carbon nanotube quantum dots”, *physica status solidi (b)*, vol. 252, no. 11, Sep. 2015.
- [7] R. Scheibner, M. König, D. Reuter, A. Wieck, C. Gould, H. Buhmann, and L. Molenkamp, “Quantum dot as thermal rectifier”, *New Journal of Physics*, vol. 10, no. 8, Aug. 2008, Article ID: 083016.
- [8] G. Benenti, G. Casati, K. Saito, and R. S. Whitney, “Fundamental aspects of steady-state conversion of heat to work at the nanoscale”, [Online]. Available: <https://arxiv.org/abs/1608.05595>.
- [9] R. P. Feynman, *The Feynman Lectures on Physics*. New York: Basic Books, 2003, vol. 1-2, ISBN: 9780738209241.
- [10] J. Splettstößer, “Weakly coupled quantum dots with strong onsite interaction”, private notes, Chalmers University of Technology Department of Microtechnology and Nanoscience, 2017.
- [11] Janine Splettstößer, *Scattering theory*, Private lecture, Feb. 2017.

A Probabilities and Currents in a Magnetic Field

For a single-level quantum dot in a magnetic field the energy level ε is split up in two, depending on the magnetic field B according to

$$\varepsilon_{\uparrow} = \varepsilon + \frac{B}{2} \quad \text{and} \quad \varepsilon_{\downarrow} = \varepsilon - \frac{B}{2}. \quad (48)$$

In order to present the expression for the occupation probabilities in a somewhat compact form, we introduce the following notations for the Fermi functions

$$\begin{aligned} f_{\uparrow}^{\alpha} &= f_{\alpha}(\varepsilon_{\uparrow}), & f_{\uparrow U}^{\alpha} &= f_{\alpha}(\varepsilon_{\uparrow} + U), \\ f_{\downarrow}^{\alpha} &= f_{\alpha}(\varepsilon_{\downarrow}), & f_{\downarrow U}^{\alpha} &= f_{\alpha}(\varepsilon_{\downarrow} + U), \end{aligned} \quad (49)$$

and the sum of the Fermi function multiplied with the coupling for respective reservoir

$$\begin{aligned} f_{\uparrow\Sigma} &= \sum_{\alpha} \Gamma_{\alpha} f_{\alpha}(\varepsilon_{\uparrow}), & f_{\downarrow\Sigma} &= \sum_{\alpha} \Gamma_{\alpha} f_{\alpha}(\varepsilon_{\downarrow}), \\ f_{\uparrow U\Sigma} &= \sum_{\alpha} \Gamma_{\alpha} f_{\alpha}(\varepsilon_{\uparrow} + U), & f_{\downarrow U\Sigma} &= \sum_{\alpha} \Gamma_{\alpha} f_{\alpha}(\varepsilon_{\downarrow} + U). \end{aligned} \quad (50)$$

To further increase the readability we will separate the nominator and denominator

$$P_0 = \frac{P_{0N}}{D}, \quad P_{\uparrow} = \frac{P_{\uparrow N}}{D}, \quad P_{\downarrow} = \frac{P_{\downarrow N}}{D}, \quad P_1 = P_{\uparrow} + P_{\downarrow}, \quad P_2 = \frac{P_{2N}}{D}, \quad (51)$$

where P_0 , P_1 and P_2 denotes zero, one respective two particles occupying the energy level, and P_{\uparrow} and P_{\downarrow} denotes an electron with spin up respective down occupying the energy level. The denominator D is defined as

$$D = 2\Gamma \left(\Gamma^2 - f_{\uparrow} f_{\downarrow} + f_{\uparrow} f_{\downarrow U} + f_{\downarrow} f_{\uparrow U} - f_{\uparrow U} f_{\downarrow U} \right). \quad (52)$$

Since the probabilities contain a recurring term, denoted G , we will also define this before dealing with the nominators;

$$G = f_{\uparrow} f_{\downarrow} (f_{\uparrow U} + f_{\downarrow U}) - f_{\uparrow U} f_{\downarrow U} (f_{\uparrow} + f_{\downarrow}). \quad (53)$$

With these definitions we can now present the probabilities

$$\begin{aligned} P_{0N} &= 2\Gamma^3 - 2\Gamma^2 (f_{\uparrow\Sigma} + f_{\downarrow\Sigma}) + \Gamma (2f_{\uparrow\Sigma} f_{\downarrow\Sigma} + f_{\uparrow\Sigma} f_{\downarrow U\Sigma} + f_{\downarrow\Sigma} f_{\uparrow U\Sigma} - 2f_{\uparrow U\Sigma} f_{\downarrow U\Sigma}) - G, \\ P_{\uparrow N} &= 2\Gamma^2 f_{\uparrow\Sigma} + \Gamma (f_{\downarrow\Sigma} f_{\uparrow U\Sigma} - f_{\uparrow\Sigma} f_{\downarrow U\Sigma} - 2f_{\uparrow\Sigma} f_{\downarrow\Sigma}) + G, \\ P_{\downarrow N} &= 2\Gamma^2 f_{\downarrow\Sigma} + \Gamma (f_{\uparrow\Sigma} f_{\downarrow U\Sigma} - f_{\downarrow\Sigma} f_{\uparrow U\Sigma} - 2f_{\uparrow\Sigma} f_{\downarrow\Sigma}) + G, \\ P_{2N} &= \Gamma (f_{\uparrow\Sigma} f_{\downarrow U\Sigma} + f_{\downarrow\Sigma} f_{\uparrow U\Sigma}) - G. \end{aligned} \quad (54)$$

When setting the magnetic field to zero, i.e. $B = 0$, we get the occupation probabilities

$$P_0 = \frac{1}{\Gamma} \frac{f_{\Sigma}^{-} f_{U\Sigma}^{-}}{f_{\Sigma}^{-} + f_{U\Sigma}^{-}}, \quad P_1 = \frac{1}{\Gamma} \frac{2f_{\Sigma} f_{U\Sigma}^{-}}{f_{\Sigma}^{-} + f_{U\Sigma}^{-}}, \quad P_2 = \frac{1}{\Gamma} \frac{f_{\Sigma} f_{U\Sigma}}{f_{\Sigma}^{-} + f_{U\Sigma}^{-}}. \quad (55)$$

These are shown in figure 6, and are easily understood by inspecting the different numerators. For example, P_0 is large when both f_{Σ}^{-} and $f_{U\Sigma}^{-}$ are large, i.e. the reservoirs are mostly unoccupied at both energies ε and $\varepsilon + U$. This causes the energy level to be mostly unoccupied, which is equivalent to a large P_0 .

The probabilities for $B \neq 0$, listed in equation (54), we can express particle current I_α^N and energy current I_α^E as

$$\begin{aligned}
I_\alpha^N &= \frac{\Gamma_\alpha}{\hbar} \left[(f_\uparrow^\alpha + f_\downarrow^\alpha) P_0 + (f_{\downarrow U}^\alpha + f_\uparrow^\alpha - 1) P_\uparrow \right. \\
&\quad \left. + (f_{\uparrow U}^\alpha + f_\downarrow^\alpha - 1) P_\downarrow + (f_{\uparrow U}^\alpha - 1 + f_{\downarrow U}^\alpha - 1) P_2 \right], \\
I_\alpha^E &= \frac{\Gamma_\alpha}{\hbar} \left[(\varepsilon_\uparrow f_\uparrow^\alpha + \varepsilon_\downarrow f_\downarrow^\alpha) P_0 + ((\varepsilon_\downarrow + U) f_{\downarrow U}^\alpha + \varepsilon_\uparrow (f_\uparrow^\alpha - 1)) P_\uparrow \right. \\
&\quad \left. + ((\varepsilon_\uparrow + U) f_{\uparrow U}^\alpha + \varepsilon_\downarrow (f_\downarrow^\alpha - 1)) P_\downarrow \right. \\
&\quad \left. + ((\varepsilon_\uparrow + U) (f_{\uparrow U}^\alpha - 1) + (\varepsilon_\downarrow + U) (f_{\downarrow U}^\alpha - 1)) P_2 \right].
\end{aligned} \tag{56}$$

B The Transition Matrix

The transition matrix for eigenstates in the quantum dot is given by $W = \sum_{\alpha} W_{\alpha}$, where W_{α} is the transition matrix for the reservoir α . W_{α} is a combination of the matrices for particles tunneling into and out of the dot, $W_{\alpha} = W^{\alpha+} + W^{\alpha-}$, and is given by

$$\begin{aligned}
 W_{\alpha} &= \begin{bmatrix} W_{0,0}^{\alpha} & W_{0,\uparrow}^{\alpha} & W_{0,\downarrow}^{\alpha} & W_{0,2}^{\alpha} \\ W_{\uparrow,0}^{\alpha} & W_{\uparrow,\uparrow}^{\alpha} & W_{\uparrow,\downarrow}^{\alpha} & W_{\uparrow,2}^{\alpha} \\ W_{\downarrow,0}^{\alpha} & W_{\downarrow,\uparrow}^{\alpha} & W_{\downarrow,\downarrow}^{\alpha} & W_{\downarrow,2}^{\alpha} \\ W_{2,0}^{\alpha} & W_{2,\uparrow}^{\alpha} & W_{2,\downarrow}^{\alpha} & W_{2,2}^{\alpha} \end{bmatrix} \\
 &= \begin{bmatrix} -f_{\uparrow}^{\alpha} - f_{\downarrow}^{\alpha} & & 1 - f_{\uparrow}^{\alpha} & & 1 - f_{\downarrow}^{\alpha} & & 0 \\ & f_{\uparrow}^{\alpha} & & f_{\uparrow}^{\alpha} - f_{\downarrow U}^{\alpha} - 1 & & 0 & & 1 - f_{\downarrow U}^{\alpha} \\ & & f_{\downarrow}^{\alpha} & & & f_{\downarrow}^{\alpha} - f_{\uparrow U}^{\alpha} - 1 & & 1 - f_{\uparrow U}^{\alpha} \\ & & & 0 & & & f_{\uparrow U}^{\alpha} & & f_{\uparrow U}^{\alpha} + f_{\downarrow U}^{\alpha} - 2 \end{bmatrix}, \tag{57}
 \end{aligned}$$

with notations from equation (49).